

Realization And Efficiency Evaluation Of A Micro-Photocatalytic Cell Prototype For Real-Time Blood Oxygenation

Marco RASPONI^{1,2,*}, Tania ULLAH², Richard GILBERT², Gianfranco B. FIORE¹, Todd THORSEN²

* Corresponding author: Tel.: +39(0)2 2399 3377; Fax: +39(0)2 2399 2260; Email: marco.rasponi@polimi.it

1: Department of Bioengineering, Politecnico di Milano, ITALY

2: Department of Mechanical Engineering, Massachusetts Institute of Technology, USA

Abstract A novel approach to blood oxygenation is presented. Microfluidic channels molded out of PDMS (using standard soft lithography techniques) work as photocatalytic cells, where the coupling of anatase titanium dioxide (TiO₂) thin films and platinum electrodes, allow an electrically assisted photocatalytic reaction to produce dissolved oxygen gas from the water content of the flowing blood. The thin films were deposited onto quartz glass substrates at room temperature (300K) using reactive RF sputtering with a Ti metal target. The results of the current study, as a proof of concept, have shown that the device can generate oxygen at a rate of 4.06×10^{-3} mM O₂/(cm² min) and oxygenate venous blood to the oxygen saturation level of arterial blood.

Keywords: Photocatalytic Cell, TiO₂, Blood oxygenation, Electrochemically Assisted Photocatalysis

1. Introduction

The breakthrough work of Fujishima and Honda in 1972 (Fujishima and Honda 1972), in which they achieved ultraviolet light-induced water cleavage with the use of titanium dioxide (TiO₂) in an electrochemical cell, has drawn considerable attention in recent years to the “acceleration of a photoreaction by the presence of a catalyst” (Mills and Le Hunte 1997) or photocatalysis. Photocatalysts work by the following principle: the material absorbs energy from photoexcitation, leading to the creation and separation of electrons and holes. Such a charge separation can generate electrical work through an external load or can be used to drive chemical (redox) reactions (Yoshihisa 2002). Research on photocatalysis has explored the decomposition of organic pollutants and microorganisms, the superhydrophilic self-cleaning properties of surfaces, and the photosplitting of water, among other applications. Semiconductors can act as photocatalysts because of their electronic structure and TiO₂, in particular, has been a popular choice. It is non-toxic and mechanically stable, can be fabricated at low-cost, and the anatase phase of TiO₂ has a

bandgap of approximately 3.2 eV, ideal for excitation by light in the ultraviolet range.

In the last few years, researchers have been investigating the effects the photocatalytic activity of TiO₂ has on blood (Monzyk, Burckle, Carleton et al. 2006; Gilbert, Carleton, Dasse et al. 2007; Subrahmanyam, Arokiadoss and Ramesh 2007a; Subrahmanyam, Ramesh and Ramakrishnan 2007b). In particular, blood oxygenation can be obtained by splitting water molecules contained in plasma and thus allowing the combination of O₂ with hemoglobin molecules. In a previous work (Monzyk et al. 2006), a photocatalytic cell (PC) was developed, which was able to oxygenate bovine blood. More recently, a simpler PC was designed and used with human blood (Subrahmanyam et al. 2007b), even if the oxygenation was reached in static conditions.

This novel approach can be used to oxygenate whole blood and treat patients with chronic and end-stage lung disease. Current therapies include transplantation and technologies that provide respiratory support—devices like the extracorporeal membrane oxygenator (ECMO). These devices rely on gas-permeable membranes to

deliver oxygen to red blood cells (RBCs) and can, unfortunately, lead to significant coagulation and hemolysis. Our goal is to create a self-contained, mobile oxygen supply suitable for implantation in patients with acute lung disease that will reduce such complications. In particular, in the present work we focused on the realization of a highly efficient PC, able to continuously oxygenate venous blood under steady-state conditions.

2. Methods

The photocatalytic cell is composed of (1) a microfluidic channel molded out of polydimethylsiloxane (PDMS); (2) a platinum electrode that is exposed to the blood flowing through the channel and by means of which a bias potential can be maintained; and (3) an anatase TiO_2 thin film deposited onto a conducting indium tin oxide (ITO) thin film to form a semiconducting junction of TiO_2/ITO .

A bias potential is maintained across the height of the channel by means of the Pt electrode, deposited as thin film onto the PDMS that comprises the top of the channel, and the ITO film that is beneath the TiO_2 (refer to Figure 1). Studies have found that the photocatalytic efficiency can be increased by creating ITO/TiO_2 junction. Applying a bias voltage across the ITO/TiO_2 junction enhances the migration of electron/hole pairs to the surface of the TiO_2 film where further oxidation of water can take place. The bias voltage also conducts away the electrons generated when the TiO_2 film is irradiated by UV light and minimizes the recombination process of electron and holes that can slow down the photocatalytic reaction (Vinodgopal and Kamat 1996; Kesselman, Lewis and Hoffmann 1997; Ku, Lee and Wang 2006).

2.1 Photocatalytic cell (PC) construction

PDMS microchannels

The photocatalytic reaction takes place in the flowing blood within a specifically designed cell, whose design relies on a very thin rectangular cross-sectioned channel (4.5mm wide x 25mm long x 0.1mm high).

The microchannel was molded in

PDMS using established soft lithography methods (Xia and Whitesides 1998). The silicon molds containing the outlines of the channel in positive relief were fabricated by spinning negative photoresist (SU8-50; MicroChem) onto silicon wafers followed by exposure to UV-radiation through a transparency mask printed with the channel outlines. The molds were pretreated with a silanizing agent (chloro-trimethyl-silane, Aldrich) and PDMS (Sylgard 184, Dow Corning) (10:1 ratio of elastomer to curing agent) was spun onto them to a thickness of $100\mu\text{m}$. After curing for 3 hours at 80°C , the solidified PDMS within the channel region was peeled away to create a void through which the fluid can flow. When assembling the device, this PDMS “gasket” was sandwiched between the platinum electrode and the glass substrate to form an enclosed channel.

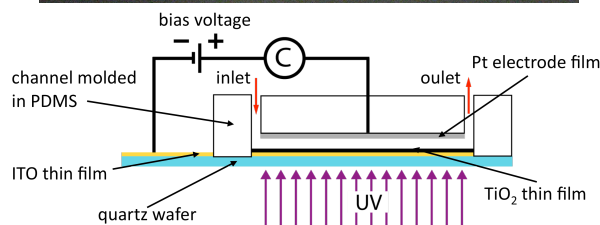
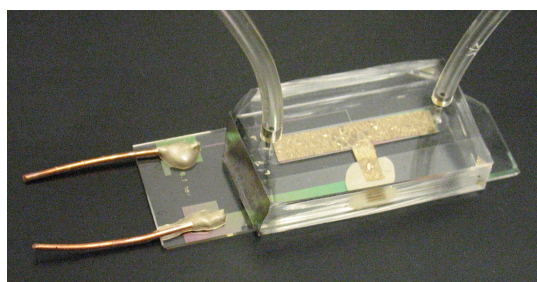


Fig. 1. Top panel: picture of the assembled photocatalytic cell schematics of (A) the microfluidic device and experimental set-up, and (B) the patterned deposition of ITO and TiO_2 thin films. The TiO_2 thin film is deposited over a $25\text{mm} \times 4.5\text{mm}$ area where it will be exposed to the fluid in the channel of the same geometry.

Platinum Electrode

In order to apply the bias voltage across the ITO/TiO_2 junction, a platinum electrode ($25\text{mm} \times 4.5\text{mm}$) was deposited on PDMS. This patterned electrode is exposed to the flowing fluid and therefore has the same length and width as the channel. To fabricate the electrodes, pieces of PDMS (25mm wide x 35mm long x 5mm thick) were prepared using elastomer and curing agent mixed to a ratio of

5:1, respectively, and baked overnight at 80°C. These thick pieces served as substrates for the metal deposition, during which further thin PDMS layers (~0.5mm) were used as masks. The primary metal composing the electrode is Pt. However, because Pt adheres poorly to PDMS, a thin layer of Ti was deposited on the substrate first (Al Mamun and Dutta 2006). An MRC sputtering system was used to deposit ~30 nm Ti and ~320 nm Pt. The PDMS mask was removed to reveal the patterned electrode.

In order to assembly, the thick PDMS (with the electrode) and the microchannel were aligned and plasma bonded.

ITO/TiO₂ thin film deposition

The ITO and TiO₂ thin films were patterned onto 3-inch quartz wafers (Mark Optics Incorporated, Santa Ana, California) which serve as the substrates for the microfluidic devices. It is necessary to pattern the films to ensure adhesion between the PDMS and the quartz, while still exposing channels to the maximum surface area of TiO₂ film. Positive photoresist (AZ 4620, Shipley) was spun onto the wafers to a thickness of 10 μm. After UV exposure through a transparency mask, the wafers were developed to reveal the photoresist pattern, washed with deionized water, and dried under nitrogen gas.

The quartz wafers were then placed in an RF sputtering system equipped with an ITO target and a thin (~200nm) film of the oxide was deposited onto the unmasked regions of the wafer. Prior the TiO₂ film deposition, the regions hosting the electrical connections were masked with an additional photoresist layer.

The TiO₂ thin film was deposited at room temperature using reaction RF magnetron sputtering with a metal Ti target. The substrates were placed in an evacuated deposition chamber, and O₂ and Ar gas (volumetric ratio 1:5, respectively) were introduced by mass flow controllers until the chamber pressure reached 1.5 mTorr. At a constant power of 300W, a 50nm TiO₂ film required a sputtering time of 75 min. A sample holder, rotating at a rate of 30 rpm, ensured that the film thickness was uniform across the wafer.

The photoresist lift-off was

accomplished by placing the wafers in an acetone bath within an ultrasonicator. The clean wafers were then annealed for 1 hr in a furnace maintained at 450°C and with a controlled inert atmosphere (N₂ gas), thus ensuring the crystallization to anatase phase. The TiO₂ thin films were characterized for crystallinity and phase, after deposition on silicon substrates, by performing glancing X-ray diffraction (GIXRD). Figure 2 shows the typical diffraction patterns of films prior to (A) and after (B) the annealing step. The peaks at characteristic angles indicate that the annealing process leads to the formation of an anatase single-phase structure.

Following annealing, the glass wafers patterned with the ITO and TiO₂ thin films were cut to obtain substrates for three identical chips.

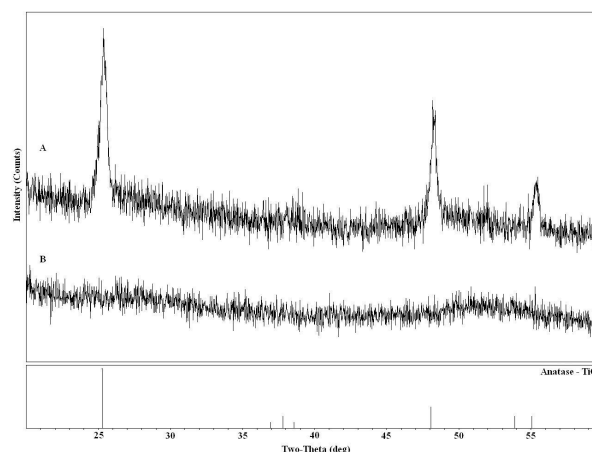


Fig. 2. The glancing incidence X-ray diffraction (GIXRD) pattern of a 50 nm TiO₂ film that has been annealed for 1 hour at 450°C (A) and one prior to the anneal step (B). The bottom portion of the graph shows the expected peak locations and relative peak intensities for pure anatase TiO₂.

Photocatalytic cell assembly

The photocatalytic cell was finally assembled by bonding the PDMS substrate (containing the Pt/Ti electrode and the molded microchannel) to the quartz chip. Prior to bonding, two holes (1.2mm diameter) were punched into the PDMS to provide inlet and outlet ports. A picture of the assembled device is shown in Figure 1 (top panel).

2.2 Experimental setup and measurement method

Figure 1 shows the experimental setup used to

perform blood oxygenation tests. The flow is driven by a syringe pump connected to the channel inlet through thick wall Tygon tubing (Cole-Parmer, 1.4mm inner diameter, ~250mm long) and steel pins (New England Small Tube Corp). A UV mercury lamp with a peak wavelength of 365 nm (BlueWave® 50 AS UV Curing Spot, Dymax Corporation, Torrington, CT) illuminates the device from underneath through a lightguide (inner diameter 5mm) placed at a distance of 75 mm. The intensity of light reaching the device is approximately 3.6 mW/cm^2 . The fluid is collected in plastic vials partially pre-filled with oil to prevent gas diffusion into and out of the samples during their filling.

Photocatalytic activity measurements

As a mean of testing the photocatalytic activity of the device prior to blood experiments, an aqueous redox indicator was used as working fluid. Methylene blue (MB, $\text{C}_{16}\text{H}_{18}\text{ClN}_3\text{S}$, Aldrich) was diluted with DI water to an initial concentration of $1 \mu\text{M}$ and pumped through the device. The MB dye is initially blue, but under photocatalytic action it degrades and loses its color. A SpectraMax M2e spectrophotometer (Molecular Devices, Sunnyvale, CA) was used to measure the concentration of the dye. Figure 3 shows the results of MB decoloration, obtained when MB was pumped through the device at different flow rates and under bias voltages ranging from no bias to 5V bias. The residence time, or the time a fluid particle resides in the channel, ranges from 7.5s ($100 \mu\text{l/min}$ flow rate) to 150s ($5 \mu\text{l/min}$ flow rate). The data shows that the concentration of MB in the flow chamber decays exponentially over time, indicating that the oxidative capacity of the device is constant over time (Kuo and Ho 2001).

2.3 Blood tests

Bovine blood obtained from a slaughterhouse (Blood Farm, Groton, MA) was used for subsequent experiments. The blood was about 36 hours old and treated as follows: A solution of 50,000 units heparin in 100 ml sterile Dextrose (5%) was combined with approximately 400 ml of blood obtained from

a single cow. The blood was then gently stirred to incorporate the heparin into the fresh blood. In a previous work (Gilbert, Park, Rasponi et al. 2007), the same procedure was used guaranteeing an activated clotting time (ACT) of approximately 400 seconds at room temperature, an accepted value for a cardiopulmonary bypass procedure (Hattersley 1966; Litwin, Mitra, Voncolditz et al. 1981; Ferguson 1995; Hirsh, Warkentin, Raschke et al. 1998; Belanger and Marois 2001).

Tests were performed with blood flowing at a constant flow rate of $12.5 \mu\text{l/min}$, corresponding to a residence time within the cell of 60 seconds. Five different initial conditions, based on various hemoglobin saturation levels, were considered. For each experimental condition, the blood in the syringe was tested through a commercial blood gas analyzer (ABL 520, Radiometer, Denmark) for hemoglobin saturation level (sO_2 [%]), pH, carbon dioxide partial pressure (pCO_2 [mmHg]), oxygen partial pressure (pO_2 [mmHg]) and hemoglobin concentration (tHb [g/dL]). The blood was then pumped through the microfluidic device and 3 blood samples ($150 \mu\text{l}$ each) were collected for another round of testing with the blood gas analyzer.

3. Results and Discussion

The decomposition rate of an organic compound such as the MB is widely considered to be a good estimate for the efficiency of TiO_2 photocatalytic activity (Matthews 1989; Lakshmi, Renganathan and Fujita 1995; Houas, Lachheb, Ksibi et al. 2001; Zhang, Oyama, Aoshima et al. 2001; Lachheb, Puzenat, Houas et al. 2002). Figure 3 shows the color removal efficiency of MB solution in terms of residence time (which is inversely proportional to the flow rate). Each curve in the figure represents the color removal undergoing a different applied bias voltage. The pure photodecomposition is quite slow, removing about 20% of the color at a flow rate of $12.5 \mu\text{l/min}$. Through the application of external bias voltage to photocatalytic process (called electrochemically assisted photocatalytic

process or photoelectrocatalytic process), the photocatalyst acts as a photoanode, driving the photogenerated electrons and holes in opposing directions so that the charge recombination is retarded (Vinodgopal and Kamat 1996; Kesselman et al. 1997; Ku et al. 2006). It was found that the better color removal efficiency was reached by applying a bias voltage of 3V, and there was no further significant improvement.

UV rays and electrolysis themselves can induce the decomposition of MB (Panizza, Barbucci, Ricotti et al. 2007). However, tests performed at this specific purpose (not reported here) showed that no statistically significant color removal occurred at these flow rate regimes.

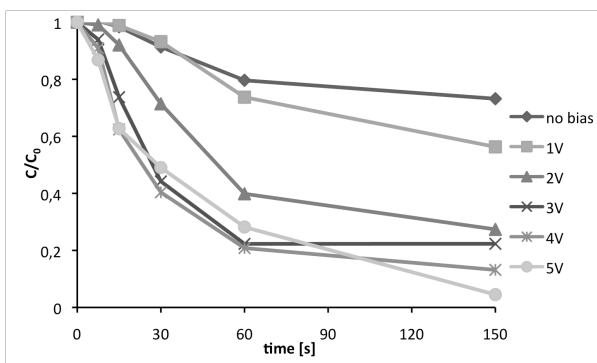


Fig. 3. Color removal tests using methylene blue solution in terms of residence time. Each curve in the figure represents the color removal under different applied bias voltages. Experiments were performed using a device with a 50nm TiO₂ thin film.

UV-induced DO production and associated changes in oxyhemoglobin concentration were measured in stabilized mixed blood at different initial oxygen concentrations and flowing at 12.5 μl/min through the test cell. At this flow rate, the resultant residence time within the cell was 60 seconds. UV exposure to the photocatalyst films resulted in almost a complete (96.60%) hemoglobin saturation in the case of using blood in physiological venous conditions (experiment S5 in Figure 4). The total oxygen content in blood (CaO₂) was calculated from the data by using the oxygen content equation:

$$CaO_2 = \kappa \cdot tHb \cdot sO_2 + \alpha \cdot pO_2 \quad (1)$$

where K is the oxygen affinity to hemoglobin ($K=1.34$ ml O₂/g Hb), α is the oxygen

solubility in blood. The resulting increase in CaO₂ was almost constant, independently of its initial value (4.06 ± 0.32 mlO₂/dl). The DO generation rate for the photocatalyst was then calculated from the data to be 8.45×10^{-5} mmol O₂/s, yielding DO flux at the photoanode of 4.06×10^{-3} mmol O₂/(cm² min).

The results clearly demonstrated that the photocatalytic reaction has the ability to fully oxygenate the blood, thus enhancing the results obtained in previous works (Dasse, Monzyk, Burckle et al. 2003; Monzyk et al. 2006), where only a partial oxygenation was reached. Higher oxygen production values were recently reported (Subrahmanyam et al. 2007a; Subrahmanyam et al. 2007b). However in (Subrahmanyam et al. 2007a; Subrahmanyam et al. 2007b), experiments were performed in a stationary environment test and the full blood oxygenation required about 2 hours. Also in our previous work (Monzyk et al. 2006), although experiments were performed in a real-time fashion and enhanced through externally applied bias voltage, the oxygen production was about 2 orders of magnitude lower than in the present work (6.25×10^{-5} mmol O₂/(cm² min) and 4.06×10^{-3} mmol O₂/(cm² min), respectively).

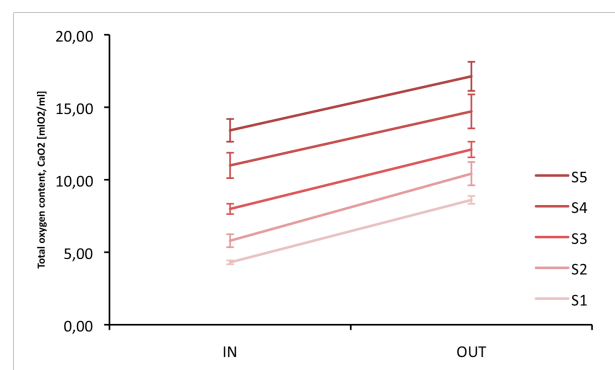


Fig. 4. Total oxygen content in bovine blood before and after the oxygenation experiments (in and out, respectively) at 5 different initial hemoglobin saturation levels by means of a blood gas analyzer.

The pH value was not altered significantly during the photocatalytic reaction, meaning that the H⁺ ions generated during the reaction were largely masked by the buffering capacity of the blood.

Moreover, the pO₂ value increased while a noticeable decrease in pCO₂ was

measured for all the 5 tested conditions. On control experiments (not reported here) where the photocatalytic chamber was substituted by a simple glass/PDMS chamber, no significant pO₂ and pCO₂ variations were registered, thus excluding the hypothesis of transport of gases through the tubing walls.

4. Conclusions

For the first time, a high efficiency flow-through device based on the photocatalytic ability of titanium dioxide to oxygenate the blood has been reported. The photocatalytic cell design presented here could be used as a readily available source of oxygen and directly oxygenate the blood bypassing the lungs. This technology could have a huge clinical impact in a wide range of acute and chronic cardiopulmonary disorders that lead to decreased tissue oxygenation. However, further studies are still needed. In particular, the geometry of the photocatalytic chamber plays a crucial role both in the reaction process (due to the effective active surface area) and in the overall hemolyticity. Moreover, the effects of UV light on blood must be carefully evaluated before an actual device can be made available for clinical use. We are currently trying to improve overall efficiency and realize a parallel integration of the channels so that the oxygen production rate can reach the physiological value.

References

- Al Mamun, N. H. and P. Dutta, 2006. Patterning of platinum microelectrodes in polymeric microfluidic chips. *Journal of Microlithography Microfabrication and Microsystems* 5(3), -.
- Belanger, M. C. and Y. Marois, 2001. Hemocompatibility, biocompatibility, inflammatory and in vivo studies of primary reference materials low-density polyethylene and polydimethylsiloxane: a review. *J Biomed Mater Res* 58(5), 467-77.
- Dasse, K. A., B. F. Monzyk, et al., 2003. Development of a photolytic artificial lung: Preliminary concept validation. *Asaio Journal* 49(5), 556-563.
- Ferguson, J. J., 3rd, 1995. Conventional antithrombotic approaches. *Am Heart J* 130(3 Pt 2), 651-7.
- Fujishima, A. and K. Honda, 1972. Electrochemical photolysis of water at a semiconductor electrode. *Nature* 238(5358), 37-8.
- Gilbert, R. J., L. M. Carleton, et al., 2007. Photocatalytic generation of dissolved oxygen and oxyhemoglobin in whole blood based on the indirect interaction of ultraviolet light with a semiconducting titanium dioxide thin film. *Journal of Applied Physics* 102(7), -.
- Gilbert, R. J., H. Park, et al., 2007. Computational and functional evaluation of a microfluidic blood flow device. *Asaio Journal* 53(4), 447-455.
- Hattersley, P. G., 1966. Activated coagulation time of whole blood. *JAMA* 196(5), 436-40.
- Hirsh, J., T. E. Warkentin, et al., 1998. Heparin and low-molecular-weight heparin - Mechanisms of action, pharmacokinetics, dosing considerations, monitoring, efficacy, and safety. *Chest* 114(5), 489S-510S.
- Houas, A., H. Lachheb, et al., 2001. Photocatalytic degradation pathway of methylene blue in water. *Applied Catalysis B-Environmental* 31(2), 145-157.
- Kesselman, J. M., N. S. Lewis, et al., 1997. Photoelectrochemical degradation of 4-chlorocatechol at TiO₂ electrodes: Comparison between sorption and photoreactivity. *Environmental Science & Technology* 31(8), 2298-2302.
- Ku, Y., Y. C. Lee, et al., 2006. Photocatalytic decomposition of 2-chlorophenol in aqueous solution by UV/TiO₂ process with applied external bias voltage. *Journal of Hazardous Materials* 138(2), 350-356.
- Kuo, W. S. and P. H. Ho, 2001. Solar photocatalytic decolorization of

- methylene blue in water. *Chemosphere* 45(1), 77-83.
- Lachheb, H., E. Puzenat, et al., 2002. Photocatalytic degradation of various types of dyes (Alizarin S, Crocein Orange G, Methyl Red, Congo Red, Methylene Blue) in water by UV-irradiated titania. *Applied Catalysis B-Environmental* 39(1), 75-90.
- Lakshmi, S., R. Renganathan, et al., 1995. Study on TiO₂-Mediated Photocatalytic Degradation of Methylene-Blue. *Journal of Photochemistry and Photobiology a-Chemistry* 88(2-3), 163-167.
- Litwin, S. B., S. K. Mitra, et al., 1981. Use of Activated Clotting Time for Monitoring Anticoagulation during Cardiopulmonary Bypass in Infants and Children with Congenital Heart-Disease. *Cardiovascular Diseases* 8(3), 364-371.
- Matthews, R. W., 1989. Photocatalytic Oxidation and Adsorption of Methylene-Blue on Thin-Films of near-Ultraviolet-Illuminated TiO₂. *Journal of the Chemical Society-Faraday Transactions I* 85, 1291-1302.
- Mills, A. and S. Le Hunte, 1997. An overview of semiconductor photocatalysis. *Journal of Photochemistry and Photobiology A: Chemistry* 108(1), 1-35.
- Monzyk, B. F., E. C. Burckle, et al., 2006. Photolytically driven generation of dissolved oxygen and increased oxyhemoglobin in whole blood. *Asaio Journal* 52(4), 456-466.
- Panizza, M., A. Barbucci, et al., 2007. Electrochemical degradation of methylene blue. *Separation and Purification Technology* 54(3), 382-387.
- Subrahmanyam, A., T. Arokiadoss, et al., 2007a. Studies on the oxygenation of human blood by photocatalytic action. *Artificial Organs* 31(11), 819-825.
- Subrahmanyam, A., T. P. Ramesh, et al., 2007b. Oxygenation of human blood using photocatalytic reaction. *Asaio Journal* 53(4), 434-437.
- Vinodgopal, K. and P. V. Kamat, 1996. Combine electrochemistry with photocatalysis. *Chemtech* 26(4), 18-22.
- Xia, Y. N. and G. M. Whitesides, 1998. Soft lithography. *Angewandte Chemie-International Edition* 37(5), 551-575.
- Yoshihisa, O. (2002). Photocatalysis: Science and Technology. a. I. O. M. Kaneko. New York, Springer: 9-28.
- Zhang, T. Y., T. Oyama, et al., 2001. Photooxidative N-demethylation of methylene blue in aqueous TiO₂ dispersions under UV irradiation. *Journal of Photochemistry and Photobiology a-Chemistry* 140(2), 163-172.